Deformation Capacity Limits for Reinforced Concrete Walls

Alex V. Shegay,[a)] M.EERI, Christopher J. Motter,[b)] M.EERI, Kenneth J. Elwood,[a)] M.EERI, and Richard S. Henry,[a)] M.EERI

The use of deformation capacity limits is becoming increasingly common in seismic design and assessment of reinforced concrete (RC) walls. Deformation capacity limits for RC walls in existing design and assessment documents are reviewed using a comprehensive database. It is found that the existing models are inconsistent and do not account for variation in deformation capacity with changes in the ratio of neutral axis depth to wall length (c/L_w) and ratio of transverse reinforcement spacing to longitudinal bar diameter (s/d_b) at the wall end region. A new mechanics-based model considering strain limits on the concrete and reinforcement is recommended. Concrete compressive strain limits for different levels of wall end region detailing are selected based on curvature ductilities for the walls in the database. Reinforcement tensile strain is limited based on a model for bar buckling. The proposed model, which accounts for c/L_w and s/d_b, is shown to have less dispersion and more accuracy than existing models when compared against experimental data and provides consistency between assessment and design provisions. [DOI: 10.1193/080118EQS193M]

INTRODUCTION

The deformation capacity of reinforced concrete (RC) walls is critical to the design of new structures as well as assessment of existing structures that utilize walls for lateral force resistance. The New Zealand (NZ) and United States standards for design and assessment take different approaches to estimate the deformation capacity of RC walls. The NZ Seismic Assessment of Existing Buildings Guideline (NZSEE 2017; referred to as the 'NZ Assessment Guideline' hereafter) contains limits on material strains to estimate the section curvature capacity. The NZ Concrete Structures Standard, Standards New Zealand (NZS) 3101:2006 (NZS 2017), and an alternative empirical assessment model proposed by Crowe (2018) for future implementation into the NZ Assessment Guideline both prescribe the deformation limits in terms of a plastic rotation normalized by an effective plastic hinge length and index yield curvature (i.e., curvature ductility). Comparatively, the United States Seismic Evaluation and Retrofit of Existing Buildings standard, American Society of Civil Engineers (ASCE) 41-17 [ASCE/Structural Engineering Institute (SEI) 2017], prescribes plastic rotation demand limits directly. ACI 318-14 [American Concrete Institute (ACI) 2014], the United States concrete design standard, does not impose specific limits on plastic rotation or curvature demand but does require that a Special Boundary Element (SBE) be provided if

[a)] Department of Civil and Environmental Engineering, University of Auckland, Auckland, New Zealand; Email: alex.shegay@auckland.ac.nz (A. V. S.)
[b)] Department of Civil and Environmental Engineering, Washington State University, Pullman, WA

the plastic rotation demand (estimated from the design roof drift ratio) is such that the extreme concrete compression fiber exceeds a strain (ε_c) of 0.003 (Wallace and Orakcal 2002). There is no deformation capacity check for walls after the SBE limit is triggered; however, recent research has proposed empirical global drift models to address this issue (Abdullah and Wallace 2019).

The curvature ductility limits implemented in NZS 3101:2006 [NZS 2006; with subsequent updates in Amendments 2 (NZS 2008) and 3 (NZS 2017)] were derived from a limited data set (Dhakal and Fenwick 2008). These limits, as well as the limits in ASCE 41-17, have not been verified against newly available wall test data. Recent testing of flexure-controlled RC walls has revealed that large drift capacities (in excess of 2.5%), corresponding to large curvature ductility capacities in the plastic hinge region, can only be achieved for walls with specific reinforcement detailing and loading conditions (Hube et al. 2014, Tran and Wallace 2015, Lu et al. 2018, Segura and Wallace 2018, Shegay et al. 2018). Parameters such as axial load, shear span ratio, shear stress demand, and end region transverse reinforcement ratio and spacing can all have a significant influence on the curvature ductility capacity of plastic hinge regions. The three ductility classes in NZS 3101:2006 and categorical limits in ASCE 41-17 are intended to broadly capture these parameters; however, the variability within each class or demand category can be substantial. In this paper, this variability is examined with respect to existing design and assessment limits as well as experimental RC wall data.

COMPARISON OF EXISTING DEFORMATION LIMITS

Deformation limits and prescribed plastic hinge lengths for RC walls from NZS 3101:2006, the NZ Assessment Guideline, ASCE 41-17, and Crowe (2018) and the trigger in ACI 318-14 for SBEs are provided in Table 1. It is evident from Table 1 that the existing standards and guidelines use different approaches to determine the plastic rotation limit. NZS 3101:2006 prescribes curvature ductility (K_d) limits for structural elements in terms of three ductility classes: Nominally Ductile, Limited Ductile, and Ductile. The K_d limits for each class were determined in a study by Dhakal and Fenwick (2008) from a limited data set consisting of only seven Ductile walls (four of which were coupled or in a dual system) and 20 singly reinforced walls classified as Nominally Ductile based on NZS 3101:2006. The NZ Assessment Guideline specifies that the maximum available curvature be determined through a plane-section moment-curvature analysis with imposed strain limits on the steel and concrete materials. The ASCE 41-17 plastic rotation limits are based on specific categories of shear stress demand, level of confinement, axial load, and demand in the compression zone. Comparatively, ACI 318-14 has two triggers for additional confinement detailing in the end region based on (1) the end region reinforcement ratio and (2) critical ratio of neutral axis length to wall length (based on the extreme concrete compression fiber exceeding a strain demand of 0.003) but no limits on the plastic hinge rotation. ACI 318-14 does not include a check to verify that the detailing in the plastic hinge can provide sufficient deformation capacity to satisfy expected rotational demands. It is clear from Table 1 and the above discussion that the method for assessing the deformation capacity of existing buildings is inconsistent with the deformation demand limits used in design of new buildings, both in NZ and the United States.

Table 1. Deformation capacity limits summary for RC walls

	Confined end region	Unconfined end region	Notes
NZS 3101:2006			
Nominally Ductile	$K_d = \text{N/A}$	$K_d = 4$	$\theta_p = K_d L_p \phi_y - \theta_y$
Limited Ductile	$K_d = 9$	$K_d = \text{N/A}$	where
Ductile	$K_d = 16$	$K_d = \text{N/A}$	$\phi_y = 2\varepsilon_y / L_w$
			$L_p = min\begin{cases} 0.15M/V \\ 0.5L_w \end{cases}$
NZ Assessment Guideline			
Concrete strain limit, ε_{cm}	$min\begin{cases} 0.004 + \frac{0.6\rho_{st} f_{yh} \varepsilon_{su}}{f'_{cc}} \\ 0.05 \end{cases}$	0.004	$\theta_p = (\phi_{cap} - \phi_y) L_p$
			$L_p = k h_{eff} + 0.1 L_w + L_{sp}$
Steel strain limit, ε_{sm}	$min\begin{cases} 0.6\varepsilon_{su} \\ 0.06 \end{cases}$	$min\begin{cases} 0.6\varepsilon_{su} \\ 0.06 \end{cases}$	
Curvature capacity, ϕ_{cap}	$min(\frac{\varepsilon_{cm}}{c}, \frac{\varepsilon_{sm}}{d-c})$	$min(\frac{\varepsilon_{cm}}{c}, \frac{\varepsilon_{sm}}{d-c})$	
Crowe (2018)			
	N/A	$K_d = 15 - 20\frac{c}{L_w}$	$\theta_p = K_d L_p \phi_y - \theta_y$
			$L_p = k h_{eff} + 0.1 L_w + L_{sp}$
ASCE 41-17[a]			
$c/L_w \le 0.18$	$\theta_p = 0.020$	$\theta_p = 0.015$	All values for $V_u / A_g \sqrt{f'_c} \le 4$ psi
$c/L_w \ge 0.45$	$\theta_p = 0.012$	$\theta_p = 0.005$	Linearly interpolated for c/L_w ranges in between
			$L_p = 0.5 L_w$
ACI 318-14			
	No limit	$\theta_p \le \frac{1}{600(1.5\frac{c}{L_w})}$[b]	$L_p = 0.5 L_w$

Note: K_d = curvature ductility = $\phi_p / \phi_y + 1$; ϕ_p = plastic curvature capacity in plastic hinge; ϕ_y = yield curvature; ε_y = yield strain of the longitudinal reinforcement not exceeding 0.0021; θ_p = plastic rotation limit; θ_y = elastic rotation at top of plastic hinge (determined by integrating the linear yield curvature profile); L_p = estimated plastic hinge length; M/V = base moment to base shear quotient; L_w = wall length; ε_{cm} = concrete compressive strain limit; ε_{sm} = reinforcement tension strain limit; ε_{su} = strain at ultimate stress of the reinforcement; ρ_{st} = volumetric ratio of confinement reinforcement in the confined end region; f_{yh} = yield stress of the confinement reinforcement; f'_{cc} = confined compression strength of concrete; ϕ_{cap} = section curvature capacity; c = neutral axis length determined at $\varepsilon_c = 0.004$; d = effective depth of longitudinal tension reinforcement; $k = 0.2(f_u/f_y - 1) \le 0.08$; $L_{sp} = 0.022 d_b f_y$ Priestley et al. (2007); f_u = ultimate stress of the longitudinal tension reinforcement; f_y = yield stress of the longitudinal reinforcement; h_{eff} = effective height of the wall; d_b = diameter of the longitudinal reinforcement; V_u = peak base shear demand; A_g = gross cross-sectional area of the wall; f'_c = unconfined compression strength of concrete; δ_u = design roof displacement; h_w = wall height; ρ_l = longitudinal reinforcement ratio in the wall end region.

[a] Conversion from ASCE 41-17 limits to c/L_w assumed a Whitney stress block factor of $\beta = 0.65$.

[b] $\theta_p = \delta_u / h_w$ assumed consistent with derivation in Wallace and Orakcal (2002).

From Table 1 it is evident that some of the plastic rotation limits specified in existing guidelines are dependent on the loading, detailing, and geometry of the wall being assessed or designed. Therefore, the graphical comparison of the plastic rotation limits from all five methods provided in Figure 1a and Figure 1b, are plotted for representative 'confined' (Shegay et al. 2018) and 'unconfined' wall cross sections (Alarcon et al. 2014, Hube et al. 2014), respectively. The limits are plotted for a range of neutral axis length to wall length ratios (c/L_w) that accounts for various axial loads and reinforcement ratios. Although the limits shown in Figure 1 are unique to the wall cross sections shown in Figure 1, the trends for each limit and relative magnitudes between limits are similar for other wall cross sections.

In Figure 1a, the NZS 3101:2006, NZ Assessment Guideline, and ASCE 41-17 limits are all similar at c/L_w ratios below 0.2. At higher c/L_w ratios, these limits diverge with the NZS 3101:2006 expression, allowing for significantly higher plastic rotation demands than the NZ Assessment Guideline and ASCE 41-17 limits. Ideally, the design limits should be lower than the assessment limits over the full range of demands because design limits are based on lower characteristic (conservative) estimates of deformation capacity whereas assessment limits are intended to provide a probable estimate. No deformation demand limit exists in ACI 318-14 for walls with SBEs. The difference between the limits for unconfined walls with $c/L_w \leq 0.2$ in Figure 1b is more pronounced than those for confined walls in Figure 1a, except for the NZS 3101:2006 and NZ Assessment Guideline limits. The NZ Assessment Guideline limits and ACI 318-14 trigger for SBEs are the lowest of the group for most c/L_w values. The limit by Crowe (2018) is the best fit to the plotted experimental data, which is to be expected, as this is an empirically derived lower-bound limit based on a database of 16 unconfined walls (Oh et al. 2002, Su and Wong 2007, Dazio et al. 2009, Alarcon et al. 2014, Hube et al. 2014,

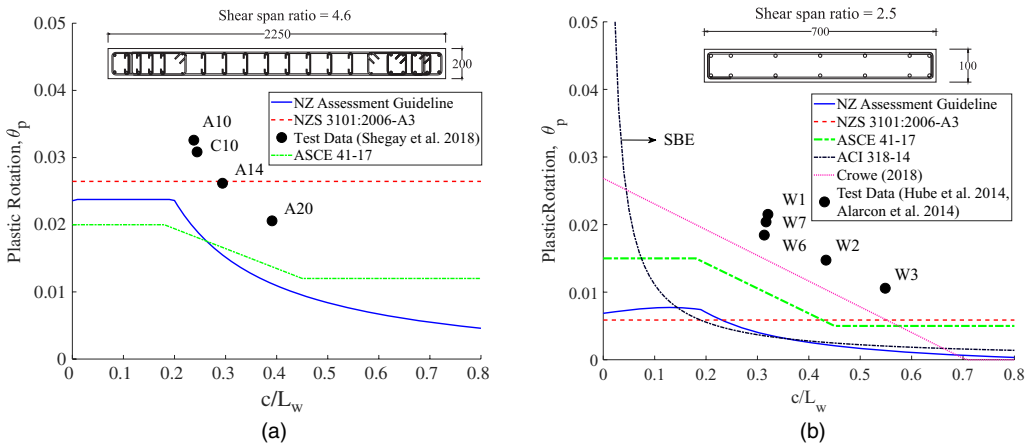

Figure 1. Comparison of limits expressed in terms of plastic rotations for (a) walls with confined end regions based on Ductile wall data from Shegay et al. (2018) and (b) walls without confined end regions based on Nominally Ductile wall data from Alarcon et al. (2014) and Hube et al. (2014).

Lu et al. 2017). Despite being developed as a lower bound, the limit by Crowe (2018) is the highest limit for $c/L_w < 0.55$ in Figure 1b, suggesting the NZS 3101:2006, NZ Assessment Guideline, and ASCE 41-17 may be overly conservative. Overall, in both Figure 1a and 1b, it is clear that the NZS 3101:2006 limits are the least representative of the trends in experimental data, being the only limits that are completely invariable with respect to c/L_w.

Several shortcomings and discrepancies exist in the deformation capacity limits in the NZ Assessment Guideline, NZS 3101:2006, and ASCE 41-17. These are summarized as follows:

1. ASCE 41-17 and NZ Assessment Guideline limits are lower than the experimental data and may be overly conservative estimates of wall deformation capacity.
2. The limits on deformation demand in NZS 3101:2006 exceed the NZ Assessment Guideline estimate of probable capacity over a wide range of c/L_w ratios, despite the conventional expectation that lower characteristic limits used for new design should typically be lower than probable values used for assessment.
3. The limits in NZS 3101:2006 are based on a very limited data set and have not been verified using a comprehensive data set that includes recent experimental data. The NZS 3101:2006 limits do not reflect the trends in the measured wall response in relation to c/L_w, unlike the NZ Assessment Guideline and ASCE 41-17.
4. The plastic rotation capacities determined based on the strain limits in the NZ Assessment Guideline have not been verified against existing data.

The above issues are the result of using limited and inconsistent data sets for the derivation of design and assessment limits. A resolution to these issues is presented in this paper in the form of a predictive model based on both empirical data and section mechanics. The proposed model is validated with a large database of applicable wall tests that accounts for a range of wall detailing parameters and demands. The resulting proposed design and assessment limits are thus unified under a common theoretical basis.

DATABASE

To assess the adequacy of deformation capacity limits in NZS 3101:2006, ASCE 41-17, and the NZ Assessment Guideline, a database of 71 wall tests from 17 studies has been compiled (see the online Appendix for details). In compiling the database for this study, a number of walls were excluded if certain criteria were not met. This was necessary to isolate walls that best represented NZ and United States (old and modern) construction and eliminate unusual cases to allow a more direct and meaningful comparison to the design and assessment limits. This study focused on walls failing in flexure, under the assumption that shear failure is mitigated through capacity design procedures in NZS 3101:2006 and considered through a separate model in the NZ Assessment Guideline and ASCE 41-17. Similarly, failure due to out-of-plane global buckling of the wall section is assumed to be properly designed for and assessed through the Paulay and Priestley (1993) model as adapted in NZS 3101:2006 and the NZ Assessment Guideline and through minimum wall slenderness requirements in ACI 318-14 (Wallace et al. 2012). Test walls were not included in the database if they met any of the following criteria: (1) splice-related failure, (2) failure in shear or out-of-plane global buckling, (3) bi-directional lateral loading, (4) shear span ratio $(\frac{M}{VL_w}) < 1.5$, (5) asymmetric/monotonic loading protocol, (6) non-constant axial load applied, and (7) longitudinal

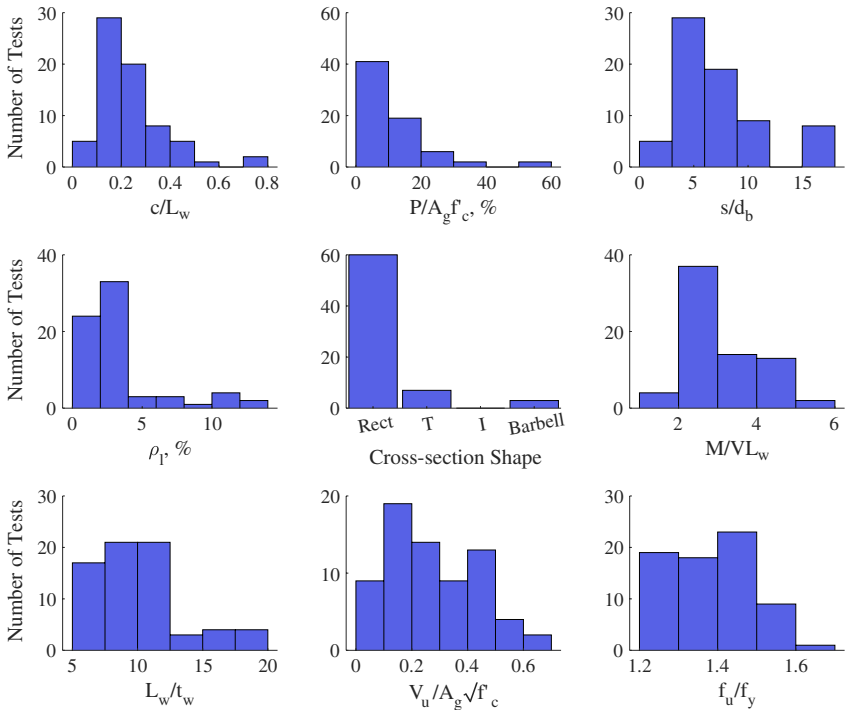

Figure 2. Summary of key wall parameters in database.

reinforcement ductility characteristics not compliant with either Standards Australia/NZS 4671 (2001) or ASTM A706/706M (2016) (hardening ratio, $\frac{f_u}{f_y}$, ≤ 1.15).

The distributions for select parameters in the database are summarized in Figure 2 with a further statistical summary provided in Table 2. The neutral axis depth was determined at $\varepsilon_c = 0.004$ from a moment-curvature analysis (using a plane-section assumption, tested material properties, and material models of Hognestad (1951) and Menegotto and Pinto (1973) for steel and concrete, respectively). Displacement capacity, δ_u, was defined as the lateral displacement at which the measured lateral load resistance first dropped below 80% of the maximum measured lateral strength.

Table 2. Summary of the database minimum, mean, maximum, and COV over a range of geometric, detailing, and demand parameters

Wall	$\frac{P}{A_g f_c'}$ [a]	$\frac{M}{VL_w}$ [b]	$\frac{V_u}{A_g\sqrt{f_c'}}$ (MPa) [c]	$\frac{L_w}{t_w}$	ρ_l [d]	$\frac{s}{d_b}$	$\frac{f_u}{f_y}$	$\frac{c}{L_w}$	$\frac{\delta_u}{h_{eff}}$ (%) [e]
Min.	0	1.5	0.045	5	0.008	1.8	1.2	0.02	1.1
Mean	0.1	2.9	0.3	10.8	0.034	6.4	1.4	0.2	2.6
Max.	0.5	6.0	0.7	18.8	0.12	17	1.6	0.7	4.4
COV (%)	96	35	56	33	83	59	8	57	30

[a]Applied axial load ratio; [b]shear span ratio; [c]shear stress demand; [d]reinforcement ratio in the boundary element; [e]drift capacity = displacement capacity normalized by effective height.

For walls where the location of the reported lateral displacement does not correspond to the effective height (h_{eff}) of the wall (e.g., tests in which moment was applied at the top of the wall), the lateral displacement at the effective height was extrapolated using an assumed cracked section bending stiffness of $0.35E_cI_g$ and shear stiffness of $0.4E_cA_g$ (where E_c is the Young's modulus of concrete, I_g is the gross cross sectional moment of inertia, and A_g is the gross cross sectional area of the wall). As the extrapolated displacement at the effective height is primarily a function of rigid body rotation (governed by measured rotation at the top of the test wall), the final computed displacements are not sensitive to the chosen values of effective stiffness. The extrapolated displacement is similarly not sensitive to the chosen values of shear stiffness because of shear demands being low for the walls that necessitated a drift correction. The database is intended to cover a realistic range of parameters that are likely to be found in practice, consistent with Figure 2. The exceptions to this are the under-representation of non-rectangular walls (limited data currently available in literature).

EVALUATION OF PROBABLE CURVATURE DUCTILITY

CURVATURE DUCTILITY DERIVATION FROM TEST DATA

To estimate the curvature ductility capacity of each wall in the database, all plastic deformation was assumed to be concentrated in the plastic hinge region at the base of the wall (lumped plasticity model), as shown in Figure 3.

The plastic rotation was calculated using geometry from Figure 3 as:

$$\theta_p = \frac{\delta_u - \delta_y}{h_{eff} - (0.5L_p - L_{sp})} \tag{1}$$

where

$$\delta_y = \frac{\phi_y h_{eff}^2}{3}$$

where δ_y is the estimated wall displacement at yield using the estimated yield curvature, ϕ_y, from Table 1. Thus, the curvature ductility can be determined for each test wall in the database using the different L_p definitions given in Table 1. Plastic hinge length definitions, provided in Table 1, corresponding to NZS 3101:2006 and the NZ Assessment Guideline, were considered, and the resulting K_d (curvature ductility) values are plotted against c/L_w, s/d_b, and shear stress demand ratios in Figure 4a and 4b, Figure 4c and 4d, and Figure 4e and 4f, respectively. Together, these three parameters capture multiple key aspects of the wall, including longitudinal reinforcement ratio, shape of the cross section, material properties, axial load ratio, effectiveness of restraint to longitudinal reinforcement buckling, and flexure-shear interaction. In asymmetrical walls (T-shapes), the larger neutral axis, associated with the direction with lower drift capacity, was reported.

Linear, ordinary least-squares regression trend lines were fitted to the data in Figure 4 with the R^2 values and standardized gradient coefficient (m) reported in the figures. The small range in absolute m-values of 0.06–2.09 indicate that the relationship between deformation capacity and either s/d_b or shear stress demand is weak, while low R^2 values

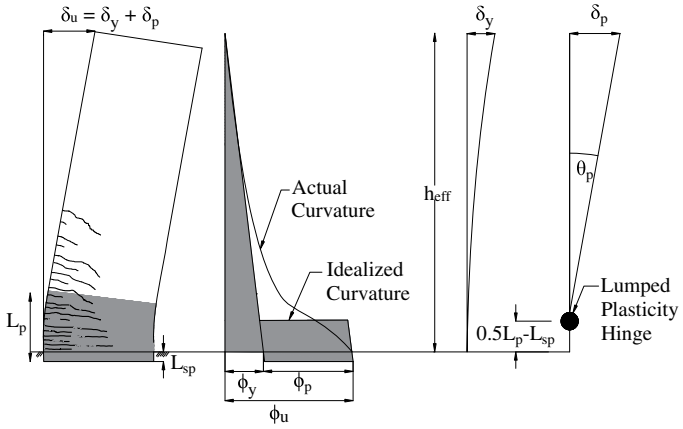

Figure 3. Lumped plasticity model based on Priestley et al. (2007).

ranging from 0.00–0.11 indicate there is significant scatter in the data. Comparatively, a stronger relationship with less dispersion is evident between curvature ductility capacity and c/L_w ratio ($R^2 = 0.33 - 0.45$ and $m = 3.93 - 4.12$). As shown in Figure 4a and 4b, the NZ Assessment Guideline plastic hinge length definition gives a higher R^2 value of 0.45 compared to 0.33 for the NZS 3101:2006 definition, while the equation for the trend line is essentially unchanged. The reduced dispersion indicates that the plastic hinge length in the NZ Assessment Guideline is more appropriate for normalizing the plastic rotations. For the remainder of the paper, the NZ Assessment Guideline plastic hinge length definition is used to estimate probable deformation capacity and derive assessment limits, and the NZS 3101:2006 plastic hinge length definition is used to derive design limits. In Figure 4a and 4b, the amount of vertical scatter in the curvature ductility capacity varies with c/L_w, suggesting that the c/L_w parameter on its own is not sufficient to explain the variation in probable curvature ductility capacity. This is expected, as the walls in the database span a wide range of transverse reinforcement detailing that includes variation in spacing, quantity, hook angle, and presence of surface deformations.

To minimize scatter, the walls in the database were grouped based on selected criteria, summarized in Table 3, for plastic hinge ductility classes of walls in NZS 3101:2006. The criteria included the transverse reinforcement spacing (s/d_b), minimum wall thickness requirements (t_{min}), and minimum longitudinal reinforcement requirements in the end region. The minimum thickness requirement was determined from §11.4.3.2 in NZS 3101:2006 (modified from Paulay and Priestley 1993) and is intended to prevent out-of-plane instability of the plastic hinge region.

The group of walls in Figure 5a met the specified criteria for the Ductile class and are hereafter referred to as Ductile walls. Figure 5b shows the remaining walls, which by default belong to either Nominally or Limited Ductile classes. There is considerable vertical scatter evident in Figure 5b ($R^2 = 0.48$), with some walls attaining curvature ductilities similar to

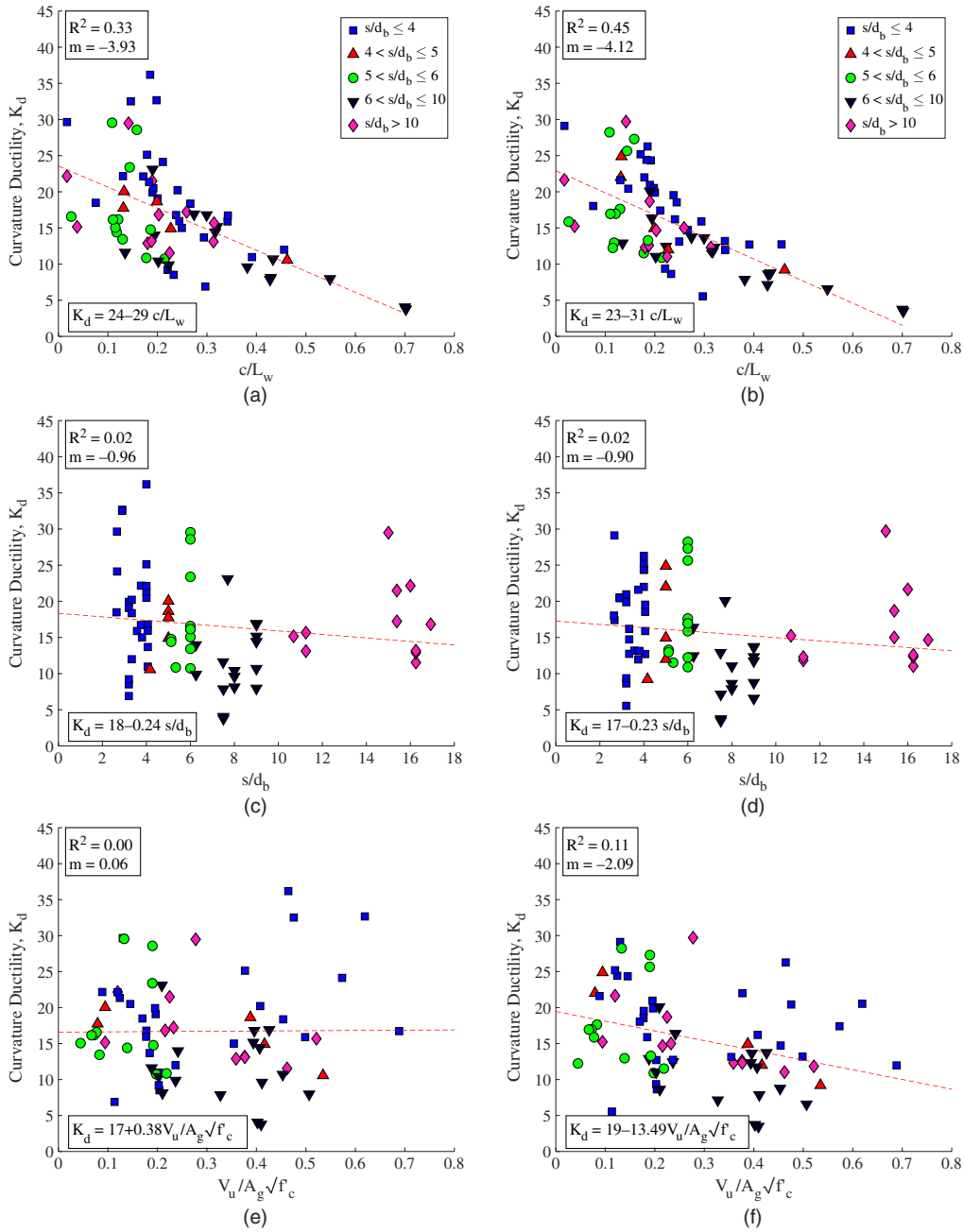

Figure 4. Curvature ductility trend for NZS 3101:2006 (left column) and NZ Assessment Guideline (right column) plastic hinge length definitions (provided in Table 1) for (a,b) c/L_w, (c,d) s/d_b, and (e,f) $V_u/A_g\sqrt{f_c'}$.

Table 3. Criteria used to differentiate wall plastic hinges of different classes

	Nominally Ductile	Limited Ductile	Ductile
$\frac{s}{d_b}$	No limit	$\frac{s}{d_b} \le 10$	$\frac{s}{d_b} \le 6$
$\rho_{l,min}$	$\rho_{l,min} \ge \frac{\sqrt{f'_c}}{4f_y}$	$\rho_{l,min} \ge \frac{\sqrt{f'_c}}{2f_y}$	$\rho_{l,min} \ge \frac{\sqrt{f'_c}}{2f_y}$
t_w	$t_w \ge t_{min}$	$t_w \ge 5t_{min}$	$t_w \ge 7t_{min}$
Confined end region	Not required	Required	Required

those in Figure 5a. This observation suggests that not meeting the Ductile plastic hinge criteria of NZS 3101:2006 does not necessarily imply that the wall will exhibit a low curvature ductility capacity. The deformation capacity of Nominally Ductile walls without many detailing requirements is expected to be less robust to such aleatory variation than that of Limited Ductile or Ductile walls. The walls in Figure 5a generally attain higher curvature ductility capacities compared to the walls with less confinement at the end regions in Figure 5b, with exception of walls with $s/d_b > 5$. As evident in Figure 5a, Ductile walls with $s/d_b > 5$ generally have lower curvature ductility than those with $s/d_b \le 5$, suggesting that s/d_b of 5 may be a more suitable design limit to differentiate walls with ductile plastic hinge regions than the current NZS 3101:2006 s/d_b limit of 6. This is supported by buckling tests on individual reinforcing bars without concrete, which, despite idealized boundary conditions, indicate that the most stable uniaxial response is achieved when the s/d_b ratio is 5 or less (Monti and Nuti 1992, Bae et al. 2005). Other studies have concluded that buckling at plastic strains can be completely eliminated at $s/d_b \le 4$ under monotonic compression loading (Bayrak and Sheikh 2001) and at $s/d_b \le 2.5$ under cyclic tension-compression loading (Rodriguez et al. 1999). Comparatively, the ACI 318-14 (2014) s/d_b limit in SBEs is never more than 6 and can be as low as 3 depending on the size and spacing of the longitudinal reinforcement in the confined end region. A trend line fit through the subset of Ductile walls

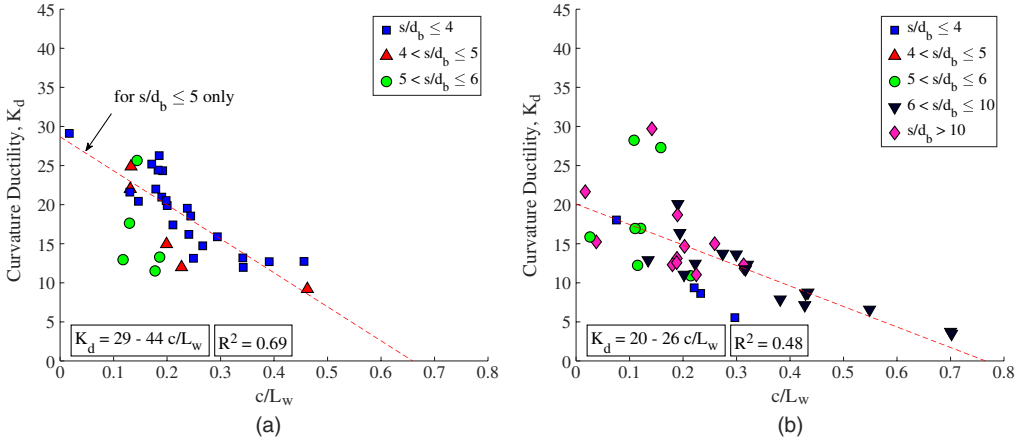

Figure 5. Walls isolated by ductility class per Table 3 and using a plastic hinge length from the NZ Assessment Guideline: (a) Ductile walls; (b) Nominally and Limited Ductile walls.

with $s/d_b < 5$ shows an improved correlation over the data set for all walls ($R^2 = 0.69$ in Figure 5a compared to $R^2 = 0.45$ in Figure 4b).

ACCURACY OF EXISTING MODELS

To benchmark the accuracy of the NZ Assessment Guideline (NZSEE 2017) and ASCE 41-17 models and the appropriateness of the NZS 3101:2006 limits for the above set of Ductile and Nominally/Limited Ductile walls, the experimentally determined curvature ductility was normalized by the curvature ductility as determined from these documents. The normalized curvature ductility was then plotted against c/L_w, s/d_b, and shear stress demand ratios as shown in Figure 6a–6c for NZ Assessment Guideline (NZSEE 2017), Figure 6d–6f for NZS 3101:2006, and Figure 6g–6i for ASCE 41-17. Normalized values above and below unity in Figure 6 indicate that the particular code/guideline underestimates and overestimates the actual curvature ductility achieved in the experiment, respectively. For assessment guidelines (in which probable capacity is sought), normalized values of unity are expected, while for design standards (in which a lower bound capacity is desired), normalized values above unity are expected. To include comparison to ASCE 41-17 (ASCE/SEI 2017) plastic rotation limits (corresponding to acceptance criteria for the 'Collapse Prevention' performance level) were converted to curvature ductility using Equation 2:

$$K_d = \frac{\theta_p}{\varepsilon_y} + 1 \tag{2}$$

This equation was derived using the ASCE 41-17 plastic hinge length assumption of $L_p = 0.5L_w$ and the NZS 3101:2006 assumption for yield curvature in Table 1. The ASCE 41-17 limits depend on end region confinement and shear stress demand. The limits were converted across a range of c/L_w values using a Whitney stress block (assuming $\beta = 0.65$).

It is evident from Figure 6 that the NZ Assessment Guideline and ASCE 41-17 limits are generally conservative (average curvature ductility capacity estimate is 1.7–2.5 times lower than the measured value for Ductile and Nominally/Limited Ductile walls), with the level of conservatism varying depending on c/L_w, s/d_b, and shear stress demand. The level of conservatism suggests that the NZ Assessment Guideline and ASCE-41-17 wall limits would be more appropriate as a lower bound than probable estimates to use in the assessment of deformation capacity. In comparison, NZS 3101:2006 provides a less conservative curvature ductility limit (average normalized limit of 1.2–1.6). Additionally, the NZS 3101:2006 limits overestimate the curvature ductility of the experimental results for 20 of the 71 walls (28% of the data) in Figure 6d–6f, compared to using the NZ Assessment Guideline and ASCE 41-17, which overestimate curvature ductility for 4 and 5 walls (6% and 7% of the data), respectively. This is consistent with the observations from Figure 1 and opposes the standard philosophy that design limits should correspond to a lower bound of the data and assessment limits should correspond to a probable curvature ductility capacity.

The accuracy of the NZ Assessment Guideline probable curvature ductility capacity, ASCE 41-17 limits, and NZS 3101:2006 limits in Figure 6 all show a level of dependency on s/d_b, c/L_w, and shear stress demand, as indicated by the absolute standardized trendline gradients (m) and associated R^2 values. The strongest dependencies are noted with respect to c/L_w in the

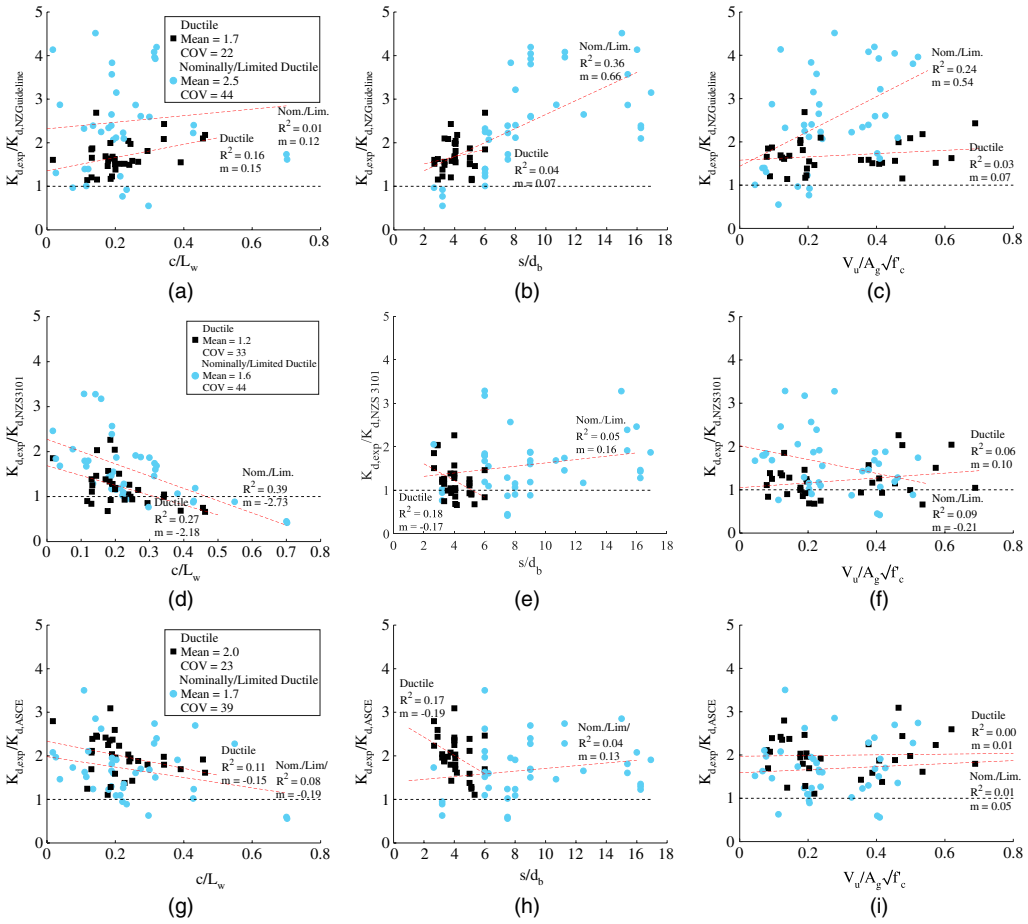

Figure 6. Curvature ductility limits for test walls relative to limits from NZ Assessment Guideline, NZS 3101:2006, and ASCE 41-17 across a range of c/L_w, s/d_b, and shear stress demand ratios. (a) NZ Assessment Guideline limits over c/L_w range; (b) NZ Assessment Guideline limits over s/d_b range; (c) NZ Assessment Guideline limits over shear stress demand range; (d) NZS 3101:2006 limits over c/L_w range; (e) NZS 3101:2006 limits over s/d_b range; (f) NZS 3101:2006 limits over shear stress demand range; (g) ASCE 41-17 limits over c/L_w range; (h) ASCE 41-17 limits over s/d_b range; (i) ASCE 41-17 limits over shear stress demand range.

NZS 3101:2006 standard ($m = 0.21$–0.43; $R^2 = 0.27$–0.39) and with respect to s/d_b and shear stress demand in NZ Assessment Guideline for Nominally/Limited Ductile walls ($m = 0.66$; $R^2 = 0.36$, and $m = 0.54$; $R^2 = 0.24$, respectively). It is evident from the trendlines and associated R^2 values that neither the design nor the assessment limits are effectively capturing the effects of the c/L_w and s/d_b parameters, which correspond to differences in curvature ductility within each ductility class as shown in Figure 5. The variation of curvature ductility with shear stress demand was also poorly captured by the NZ Assessment Guideline. The ASCE 41-17 limits are shown to suitably account for variation in deformation capacity

with shear stress demand as indicated by the small trendline gradients ($m = 0.01–0.05$) and R^2 ($R^2 = 0–0.01$) values in Figure 6i. Dispersion of the data about the mean is quantified using the coefficient of variation (COV). The COV using NZS 3101:2006 design limits (33%) is higher than the NZ Assessment Guideline limits (22%) and ASCE 41-17 limits (23%) for Ductile walls, indicating that the NZS 3101:2006 design limits are the least consistent with the experimental data. The COV for Nominally/Limited Ductile walls (39%–44%) is higher than for Ductile walls (22%–33%) for all three standards, indicating that deformation capacity of Nominally/Limited Ductile walls is estimated with less certainty than Ductile walls.

PROPOSED MODEL

A proposed curvature ductility capacity model based on mechanics is described in this section and is calibrated to fit the experimental data from the wall database. Fundamentally, the model takes a material strain-limit approach by assuming constant strains over the length of the theoretical plastic hinge. Various additional assumptions and simplifications are made in the derivation of the final limit in order to make this model easily and directly applicable to engineering practice.

CONCRETE STRAIN LIMIT MODEL

The curvature capacity of the section, ϕ_{cap}, can be expressed with Equation 3 utilizing the Navier-Bernoulli (i.e., plane sections remain plain after bending) assumption, where ε_{cm} is a concrete compression strain limit:

$$\phi_{cap} = \frac{\varepsilon_{cm}}{c} \tag{3}$$

Dividing Equation 3 by the estimate of yield curvature in Table 1, the curvature ductility capacity envelope can be expressed in terms of the extreme fiber compressive strain limit (ε_{cm}), longitudinal reinforcement yield strain (ε_y), and neutral axis to wall length ratio (c/L_w):

$$K_d = \frac{\varepsilon_{cm}}{2\varepsilon_y\left(\frac{c}{L_w}\right)} \tag{4}$$

This envelope relies on the simplifying assumption that the neutral axis length remains constant after $\varepsilon_c = 0.004$ (at which c is computed); however, it is acknowledged that the neutral axis length may fluctuate depending on cover spalling, longitudinal reinforcement strain hardening, and increased concrete strength because of confinement from transverse reinforcement. Several envelopes corresponding to different concrete strain limits are plotted in Figure 7a and 7b. Because the ultimate capacity of the section is governed by the strain in the confined end region (not in the extreme compression fiber), the true limiting strain will be slightly lower than the values of ε_{cm} shown in Figure 7. The curves in Figure 7a are plotted assuming a reinforcement tensile yield strain of $\varepsilon_y = 0.0021$, as 76% of all walls in the database use longitudinal reinforcement with a yield stress exceeding 425 MPa.

Based on Figure 7a, recommended concrete compression strain limits were determined and are provided in Table 4. It is implicit in the determination of θ_p (and subsequently K_d) for each wall that the recommended strain limits in Table 4 are assumed to be constant over the assumed plastic hinge length. A limit of $\varepsilon_{cm} = 0.018$ was found to be reasonable for the average curvature

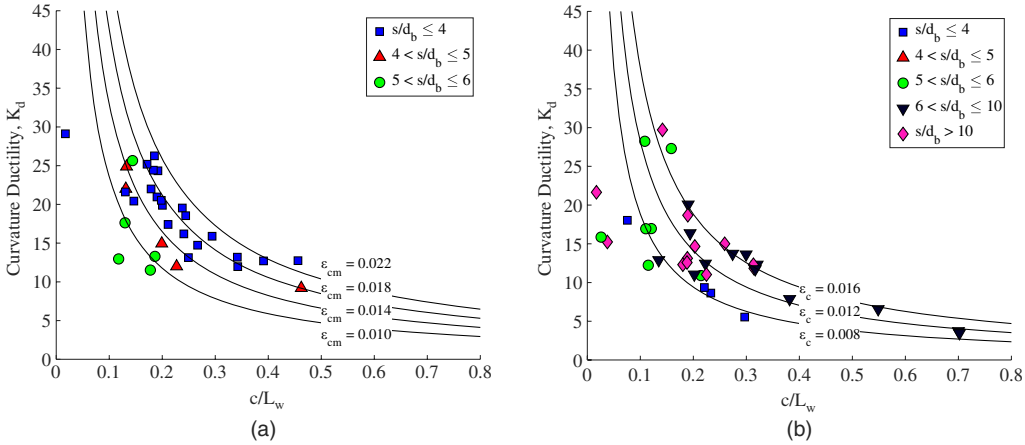

Figure 7. Curvature ductility capacity if limited only by a concrete compression strain limit. (a) Compression strain limits for Ductile walls; (b) compression strain limits for Nominally/Limited Ductile walls.

ductility capacity of Ductile walls with $s/d_b \le 4$. Welt (2015) similarly concluded from compressive tests on concrete prisms (isolated wall end regions/boundary elements) that a concrete strain capacity of $\varepsilon_{cm} = 0.020$ can be expected from prisms with ACI 318-14 SBE-level detailing and $s/d_b \le 4$. Additionally, Priestley and Kowalsky (1998) previously suggested the same concrete compressive strain limit of $\varepsilon_{cm} = 0.018$ as a reasonably conservative limit for walls detailed to NZS 3101:1995 (1999), which had similar detailing requirements to NZS 3101:2006 (2017). It is shown in Figure 7a that $\varepsilon_{cm} = 0.014$ provides a lower bound to all data with $c/L_w \ge 0.2$ and $s/d_b \le 4$ and is therefore an appropriate limit for design (walls with $c/L_w \le 0.2$ and $s/d_b \ge 4$ are addressed in the next section). For Nominally/Limited Ductile walls, it is shown in Figure 7b that concrete compressive strain limits of $\varepsilon_{cm} = 0.012$ and $\varepsilon_{cm} = 0.008$ are suitable for the mean and lower bound estimates, respectively, for walls with $c/L_w \ge 0.1$ (walls with $c/L_w \le 0.1$ are addressed in the next section). A strain limit of $\varepsilon_{cm} = 0.008$ is also used in the Chilean concrete structures design code DS 60 (Ministry of Housing and Urbanism of Chile 2011) to define the minimum curvature capacity for any level of detailing in walls.

Table 4. Concrete compressive strain limits and K_{d_max} limits for the proposed model in Equation 8

	Ductile	Nominally/Limited Ductile
Concrete strain limit for assessment (probable)	$\varepsilon_{cm} = 0.018$	$\varepsilon_{cm} = 0.012$
Concrete strain limit for design (lower bound)	$\varepsilon_{cm} = 0.014$	$\varepsilon_{cm} = 0.008$
K_{d_max}	12 for $s/d_b \ge 5$ 22 for $s/d_b \le 4$ Linear interpolation for $4 \le s/d_b \le 5$	12

The underlying assumption when using Equation 4 is that the wall curvature ductility capacity is limited by a compression failure mechanism. This is often not the case and is the reason that a number of walls in Figure 7a with $c/L_w \leq 0.2$ and/or $s/d_b \geq 4$ fall below the proposed limit. An extension to the proposed model is presented in the next section to deal with this shortcoming.

REINFORCEMENT STRAIN LIMIT

The proposed limit for curvature ductility in Equation 4, which approaches infinity with a decreasing c/L_w ratio, is based only on compression failure of concrete. In reality, at low c/L_w ratios (i.e., sections with low axial demand or low reinforcement ratio), the section ductility transitions from being governed by the compressive failure of concrete to tensile failure of reinforcement. For example, fracture of the reinforcement will result in a direct reduction of global lateral strength capacity, while buckling of the reinforcement (on reverse loading from high tension plastic strains) will result in (1) higher compressive stresses in the concrete core from redistribution and (2) compromised confinement of the concrete core. In the NZ Assessment Guideline, the reinforcement strain limit is taken as the lesser of $\varepsilon_{sm} = 0.06$ or $\varepsilon_{sm} = 0.6\varepsilon_{su}$ (where ε_{su} is the ultimate strain capacity of the reinforcement), unless the s/d_b ratio is above 6.0, in which case the buckling model by Rodriguez et al. (2013) is recommended.

Models to estimate the strain demand at initiation of reinforcement buckling have been proposed in numerous studies based on buckling mechanics and test data (Rodriguez et al. 1999, 2013, Moyer and Kowalsky 2003, Alvarado et al. 2015, Motter et al. 2018). These models all attempt to predict the strain parameter ε_{sc} for a given s/d_b. The strain parameter ε_{sc} has previously been established as a key indicator for predicting the onset of buckling (Rodriguez et al. 1999) and is defined in Figure 8 as the total strain experienced by the bar from its peak tension strain, $\varepsilon_{s,max}$, to some compressive strain, ε_c (not exceeding ε_{cm}), at which buckling is expected to occur. The maximum curvature and curvature ductility capacity associated with the buckling of reinforcement can then be defined using ε_{sc}, as in Equation 5 and 6, respectively. The relationship developed by Moyer and Kowalsky (2003) is selected to compute ε_{sc}, as its theory is based on the mechanics of bar buckling. Moyer and Kowalsky (2003) determined a relationship between ε_{sc} and s/d_b (Equation 7) based on the Euler buckling theory as modified by Engesser (1895) for a reduced modulus and the assumption that reinforcement buckling occurs strictly between ties:

$$\phi_{cap} = \frac{\varepsilon_{sc}}{L_w} \tag{5}$$

$$K_{d\_max} = \frac{\varepsilon_{sc}}{2\varepsilon_y} \tag{6}$$

$$\varepsilon_{sc} = 3\left(\frac{s}{d_b}\right)^{-2.5} \tag{7}$$

By substituting Equation 7 into Equation 6, maximum curvature ductility capacity can be determined for any value of s/d_b. Curvature ductility limits for s/d_b of 4.0, 5.0, and 6.0 are 22.0, 12.6, and 8.0, respectively (using $\varepsilon_y = 0.0021$). This is based on a conservative

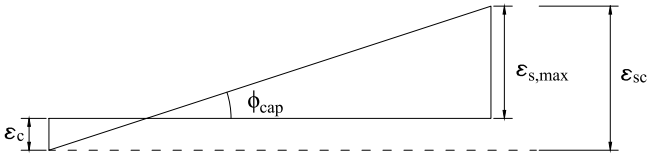

Figure 8. Definition of ε_{sc} on the wall cross-sectional strain diagram.

assumption that curvature ductility capacity is reached at the first instance of reinforcement buckling. This is not always the case for larger s/d_b ratios or low compression demands. This is demonstrated in Figure 9a and 9b, in which the drift at wall failure normalized by the drift at initial buckling (if reported) is plotted against the s/d_b ratio and c/L_w ratio, respectively. In Figure 9a it is evident that the drift at wall failure is generally higher than the drift at initiation of buckling as s/d_b increases. It is particularly noted that walls with $s/d_b \leq 4$ are much more likely to fail when buckling first occurs. This trend occurs because when the wall end region is well confined (small s/d_b), buckling compromises the confinement of concrete, which is critical to section ductility. Additionally, reinforcement buckling occurring between closely spaced hoops (small s/d_b) will result in higher localized strains in the buckled bars than if occurring over a larger effective length, which would trigger fracture and corresponding strength loss shortly thereafter. In Figure 9b it is seen that when compressive demands are low ($c/L_w < 0.2$), global failure also does not occur immediately after initial reinforcement buckling. Therefore, it is deemed that the K_{d_max} limit corresponding to an s/d_b ratio of 6 is overly restrictive, and walls are likely to sustain additional deformation after buckling is initiated. It is recommended that an upper bound of $s/d_b = 5$ ($K_{d\_max} \approx 12$) be used, as this can adequately describe the probable curvature ductility capacity for walls with $s/d_b \geq 5$.

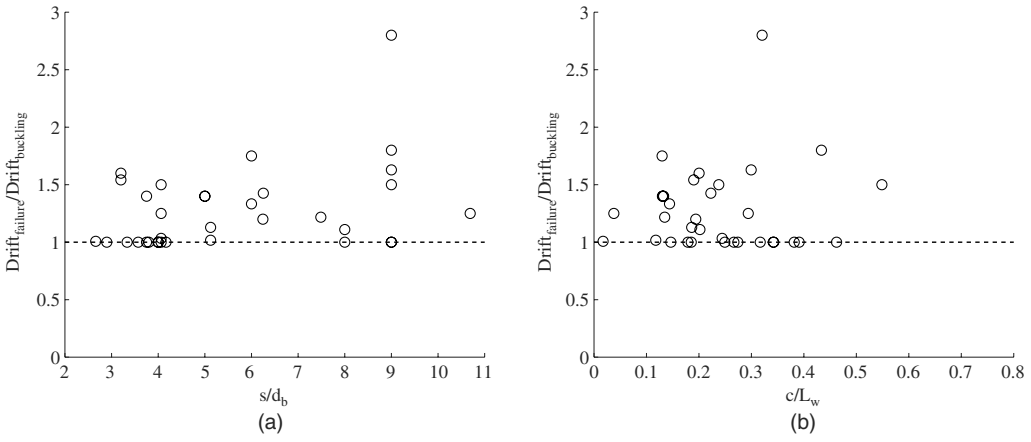

Figure 9. Ratio of drift at failure to drift at initial reinforcement buckling over a range of (a) s/d_b and (b) c/L_w values.

PROPOSED MODEL SUMMARY

By combining Equation 4 for compression failure with the reinforcement buckling criteria above, the final proposed model for the design and assessment of RC walls is provided in Equation 8 with the compression strain limits and K_{d_max} values provided in Table 4:

$$K_d = \frac{\varepsilon_{cm}}{2\varepsilon_y\left(\frac{c}{L_w}\right)} \leq K_{d\_max} \tag{8}$$

The final proposed curvature ductility capacity models are plotted with the experimental data in Figure 10, with the concrete strain controlled segment of the limit plotted in solid black and segment of the limit controlled by s/d_b ratio plotted using red horizontal dotted lines.

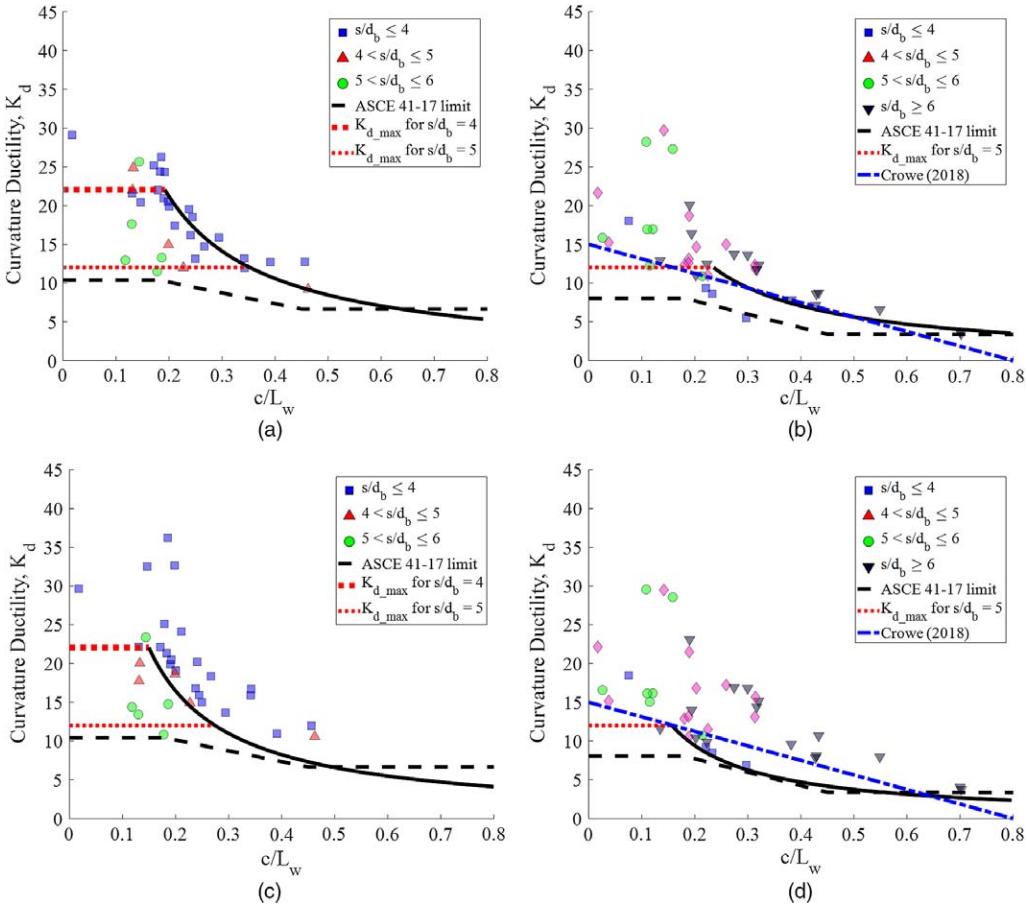

Figure 10. Proposed curvature ductility capacity limits for (a) assessment of Ductile walls, (b) assessment of Nominally/Limited Ductile walls, (c) design of Ductile walls, and (d) design of Nominally/Limited Ductile walls.

The limits in Figure 10a and 10b provide a suitable estimate to the data and are appropriate for assessment, while the limits in Figure 10c and 10d provide a suitable lower bound to the data and are appropriate as design limits. ASCE 41-17 limits are shown in Figure 10a and Figure 10c for walls with confined end regions, and in Figure 10b and Figure 10d for walls with unconfined end regions. The plotted ASCE 41-17 limits correspond to a shear stress demand ratio of $\leq 4\sqrt{f_c'}$ psi. It is evident from Figure 10a and 10b that the proposed assessment limits provide a better fit to the experimental data than the existing ASCE 41-17 limits for walls with low shear stress demand. The proposed limit by Crowe (2018) is a reasonable linear approximation to the proposed assessment model with Nominally/Limited Ductile walls, as shown in Figure 10b, but is not a suitable lower bound limit, as shown in Figure 10d. The use of $K_{d\_max} = 12$ (corresponding to $s/d_b \approx 5$) provides a suitably conservative estimate for the curvature ductility capacity of Nominally/Limited Ductile walls with $s/d_b \geq 5$ and $c/L_w \leq 0.25$.

The proposed curvature ductility limits for assessment can be converted to plastic rotation limits for integration into ASCE 41-17 using Equation 9, where L_p and ϕ_y use the NZ Assessment Guideline definitions in Table 1 and K_d is defined using Equation 8 and Table 4:

$$\theta_p = L_p \phi_y (K_d - 1) \tag{9}$$

ACCURACY OF PROPOSED MODEL

Plots of the measured curvature ductility for the test walls normalized by the value determined using the proposed model are shown in Figure 11. The normalized curvature ductility is plotted against c/L_w, s/d_b, and shear stress demand ratios in Figure 11a–11c for the probable capacity model proposed for NZ Assessment Guideline (NZSEE 2017) and in Figure 11d–11f for the lower bound model proposed for NZS 3101:2006. Because the conversion from curvature ductility to plastic hinge rotation used a consistent methodology for the proposed limit and experimental data, plots for the ratio of measured plastic rotation capacity to proposed probable plastic rotation capacity are identical to those in Figure 11. Statistical information for the existing and proposed assessment/design models is summarized in Table 5. As desired, the proposed assessment model provides an improved estimate of the probable deformation capacity compared to existing models (mean prediction accuracy of 1.1–1.3 using the proposed model compared to 1.7–2.5 using NZ Assessment Guideline model and ASCE 41-17 model). For Ductile walls, the COV using the proposed assessment model (27%) is similar to using the ASCE 41-17 and NZ Assessment Guideline models (23% and 20%, respectively), indicating that the improvement in mean prediction accuracy has come at almost no detriment to the consistency of the prediction. For Nominally/Limited Ductile walls, the consistency in prediction improved using the proposed assessment model, as evidenced by a reduction in COV for the proposed model (34%) compared to the NZ Assessment Guideline model (44%) and ASCE 41-17 model (39%).

The proposed design curvature ductility limits are conservative, as they are 1.4–1.7 times lower than experimental curvature ductility on average. However, the confidence of the prediction is improved using the proposed model compared to existing models, indicated by the reduction in COV from 33%–44% in the NZS 3101:2006 model compared to 20%–34% in the proposed model. As shown in Table 5, use of the proposed design model results in a

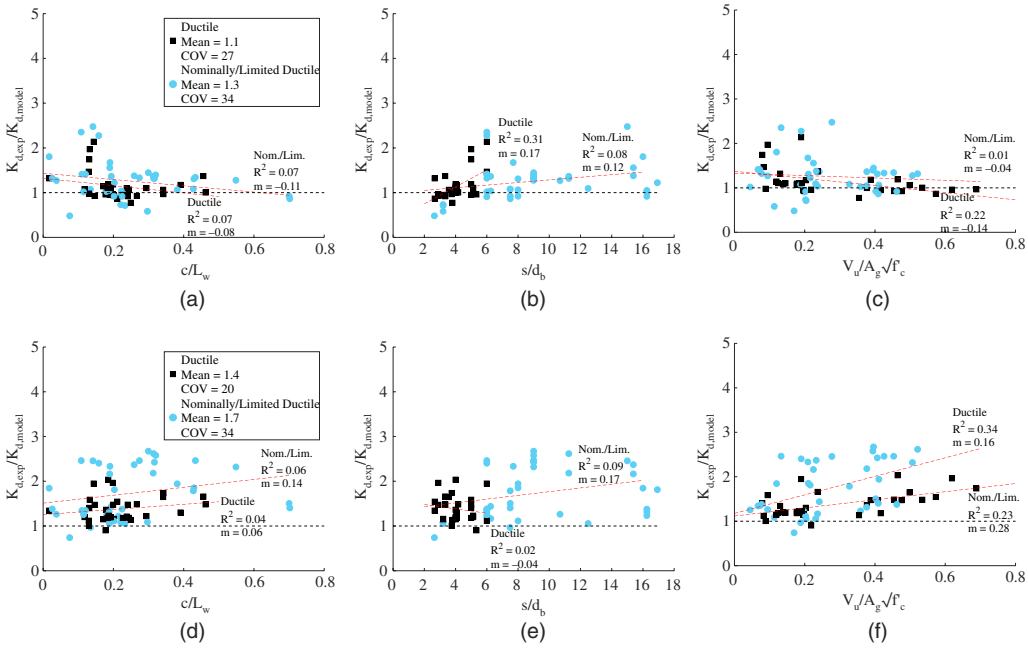

Figure 11. Measured curvature ductility capacity normalized by that estimated by the proposed model over a range of c/L_w, s/d_b, and shear stress demand. (a) Proposed model for NZ Assessment Guideline c/L_w; (b) proposed model for NZ Assessment Guideline s/d_b; (c) proposed model for NZ Assessment Guideline shear stress demand; (d) proposed model for NZS 3101 c/L_w; (e) proposed model for NSZ 3101 s/d_b; and (f) proposed model for NZS 3101 shear stress demand.

significantly smaller percentage of walls with an under-predicted curvature ductility capacity, which is critical for design purposes. The smaller gradients of the trendlines and associated R^2 values shown in Figure 11 and reported in Table 5 indicate reduced dependency of the model accuracy on s/d_b, c/L_w, and shear stress demand that was present with the existing models (see Figure 6), indicating that the proposed model adequately accounts for these parameters. The exception to this is the proposed assessment model for Ductile walls with respect to s/d_b ($m = 0.17$, $R^2 = 0.31$); however, it is evident from Figure 11b that the trend is influenced by the three largest values. The variation of curvature ductility with respect to shear stress demand has been significantly reduced in Figure 11c compared to that observed in Figure 6c, suggesting that the data set used in this study is not sensitive to shear stress demand after c/L_w and s/d_b are accounted for. It is noted that only a few test walls in this study exceed a shear stress demand of $0.5\sqrt{f_c'}$ (MPa). Walls designed in NZ typically do not exceed this value of shear stress because of capacity design requirements. Walls with a shear demand well in excess of this [for example, close to the maximum limits of $0.8\sqrt{f_c'}$ (MPa) in ACI 318-14 or $0.7–1.0\sqrt{f_c'}$ (MPa) in NZS 3101:2006] may require the use of models with explicit consideration of shear stress demand ratio, such as that by Abdullah and Wallace (2019).

Table 5. Statistical summary for existing and proposed limit models for design and assessment

	COV		Mean accuracy		R^2[a]		Trendline gradient, m[a]		% walls under-predicted	
	Duct.	Nom./Lim.	Duct.	Nom./Lim.	Duct.	Nom./Lim.	Duct.	Nom./Lim.	Duct.	Nom./Lim.
NZ Assessment Guideline	22%	44%	1.7	2.5	0.17	0.1	0.15	0.12	0%	12%
					0.04	0.36	0.07	0.66		
					0.03	0.24	0.07	0.54		
ASCE 41-17	23%	39%	2.0	1.7	0.11	0.08	−0.15	−0.19	0%	16%
					0.17	0.04	−0.19	0.13		
					0.0	0.01	0.01	0.05		
Proposed model for assessment	**27%**[b]	**34%**	**1.1**	**1.3**	**0.07**	**0.07**	**−0.08**	**−0.11**	**41%**	**38%**
					0.31	**0.08**	**0.17**	**0.12**		
					0.22	**0.01**	**−0.16**	**−0.04**		
NZS 3101:2006	33%	44%	1.2	1.6	0.27	0.39	−0.21	−0.43	31%	18%
					0.18	0.05	−0.17	0.16		
					0.06	0.09	0.1	−0.21		
Proposed model for design	**20%**[b]	**34%**	**1.4**	**1.7**	**0.04**	**0.06**	**0.06**	**0.14**	**3%**	**5%**
					0.02	**0.09**	**−0.04**	**0.17**		
					0.34	**0.23**	**0.16**	**0.28**		

[a] The top, middle, and bottom value are relative to c/L_w, s/d_b, and shear stress demand, respectively.
[b] Bold formatting highlights the statistics for the proposed design and assessments models.

The proposed model is therefore more rational for use in design and assessment compared to the current NZ Assessment Guideline and NZS 3101:2006 models. An advantage of the proposed model is that it unites the design and assessment limits under the same theoretical basis, thereby achieving consistency between the design of new buildings and assessment of existing buildings. This consistency is currently missing in both NZ and United States standards.

CONCLUSIONS AND RECOMMENDATIONS

The NZS 3101:2006 concrete design standard and NZ Seismic Assessment Guideline prescribe limits on curvature ductility for use in design and assessment of RC wall plastic hinges, respectively. Both methods were compared to experimental data from a compiled data set of RC wall tests in which curvature ductility capacity was determined assuming that all plastic deformation (taken at 20% loss of lateral load-carrying capacity) was concentrated in a theoretical plastic hinge length. Both sets of limits were found to inadequately represent the lower bound and probable curvature ductility capacity of Ductile and Nominally/Limited Ductile walls and also showed dependence on the c/L_w, s/d_b, and shear stress demand parameters. Similar conclusions were also found for plastic rotation limits in ASCE 41-17. A material-strain limit approach that considers section mechanics was used to develop an improved and unified model from which both design and assessment limits were derived.

The following conclusions are drawn from this study:

1. The calculated curvature ductility using the NZ Assessment Guideline and ASCE 41-17 limits resulted in low estimates of the probable curvature ductility capacity, with the mean experimental data to prediction ratios ranging between 1.7–2.5 for Ductile and Nominally/Limited Ductile walls. It was also shown that both sets of assessment limits and the NZS 3101:2006 design limits are highly sensitive to variability in the c/L_w and s/d_b parameters of the wall.
2. The NZS 3101:2006 and NZ Assessment Guideline provisions were found to be irrational in relative magnitude, such that the curvature ductility design limit exceeded the limit used for assessment.
3. Using plastic hinge length definitions recommended in the NZS 3101:2006 and NZ Assessment Guideline provisions, concrete compressive strain limits of $\varepsilon_{sm} = 0.018$ and $\varepsilon_{sm} = 0.014$ were found to define suitable alternative limits for the probable and lower bound curvature ductility capacity of Ductile walls. The curvature ductility is further limited by a reinforcement buckling strain limit based on s/d_b. This approach reduced the bias observed in existing models to c/L_w, s/d_b, and shear stress demand and resulted in a more accurate average estimate of the probable curvature ductility capacity.
4. Shear stress demand did not have a significant influence on the accuracy of estimates of probable curvature ductility capacity using the proposed model; however, it is acknowledged that the data set used in this study had a small representation of walls with shear stress demands above $0.5\sqrt{f'_c}$. Walls with shear stress demands in excess of this value may require explicit consideration of shear stress demand on the deformation capacity.

5. The strain limit approach was also used to define curvature ductility capacity for walls with a lower level of detailing (i.e., Nominally/Limited Ductile walls) using concrete compressive strain limits of $\varepsilon_{sm} = 0.012$ and $\varepsilon_{sm} = 0.008$ for probable and lower-bound, respectively.
6. A reinforcement tension strain limit based on s/d_b was proposed to supplement the concrete strain limits and capture tension-controlled failures. In calculating the tension strain limit, an s/d_b of 6 was found to be overly restrictive on the probable curvature ductility capacity as walls with $s/d_b > 5$ were found to be typically able to sustain additional deformation after initiation of reinforcement buckling. Therefore, K_{d_max} values are recommended based on upper and lower bounds on s/d_b of 4 and 5, respectively, with linear interpolation in between.

ACKNOWLEDGMENTS

The research presented herein was funded by the Building Performance Branch of the NZ Ministry of Business Innovation and Employment.

APPENDIX

Please refer to the online version of this manuscript to access the supplementary material provided in the Appendix.

REFERENCES

Abdullah, S. A., and Wallace, J. W., 2019. Drift capacity of reinforced concrete structural walls with special boundary elements, *ACI Structural Journal* **116**, 183–194.

Alarcon, C., Hube, M., and de la Llera, J. C., 2014. Effect of axial loads in the seismic behavior of reinforced concrete walls with unconfined wall boundaries, *Engineering Structures* **73**, 13–23.

Alvarado, I. M., Rodriguez, E. M., and Restrepo, I. J., 2015. Resistencia a flexocompresión y capacidad de deformación lateral de muros rectangulares de concreto reforzado en zonas sismicas, in *Congreso Nacional de Ingenieria Sismica*, 24–27 November, Acapulco, Mexico (in Spanish).

American Concrete Institute (ACI), 2014. *Building Code Requirements for Structural Concrete and Commentary, ACI 318-14*, Naples, FL.

American Society of Civil Engineers/Structural Engineering Institute, 2017. *Seismic Evaluation and Retrofit of Existing Buildings, ASCE/SEI 41-17*, Reston, VA.

ASTM International, 2016. *Specification for Deformed and Plain Low-Alloy Steel Bars for Concrete Reinforcement*, *ASTM A706/706M-16*, West Conshohocken, PA.

Bae, S., Mieses, A. M., and Bayrak, O., 2005. Inelastic buckling of reinforcing bars, *Journal of Structural Engineering* **131**, 314–321.

Bayrak, O., and Sheikh, S. A., 2001. Plastic hinge analysis, *Journal of Structural Engineering* **127**, 1092–1100.

Crowe, S. E., 2018. Seismic Performance of Older Reinforced Concrete Walls, Masters Thesis, University of Auckland, New Zealand.

Dazio, A., Beyer, K., and Bachmann, H., 2009. Quasi-static cyclic tests and plastic hinge analysis of RC structural walls, *Engineering Structures* **31**, 1556–1571.

Dhakal, R. P., and Fenwick, R. C., 2008. Detailing of plastic hinges in seismic design of concrete structures, *ACI Structural Journal* **105**, 740–749.

Engesser, F., 1895. Über knickfragen, *Schweizerische Bauzeitung* **25**, 88–91 (in German).

Hognestad, E., 1951. *A Study of Combined Bending and Axial Load in Reinforced Concrete Members*, University of Illinois, Urbana-Champaign, IL, 128 pp.

Hube, M. A., Marihuén, A., de la Llera, J. C., and Stojadinovic, B., 2014. Seismic behavior of slender reinforced concrete walls, *Engineering Structures* **80**, 377–388.

Lu, Y., Gultom, R. J., Ma, Q. Q., and Henry, R. S., 2018. Experimental validation of minimum vertical reinforcement requirements for ductile concrete walls, *ACI Structural Journal* **115**, 1115–1130.

Lu, Y., Henry, R. S., Gultom, R., and Ma, Q. T., 2017. Cyclic testing of reinforced concrete walls with distributed minimum vertical reinforcement, *Journal of Structural Engineering*, **143**, 04016225-1–04016225-17.

Menegotto, M., and Pinto, P. E., 1973. *Method of Analysis for Cyclically Loaded R.C. Plane Frames Including Changes in Geometry and Non-Elastic Behaviour of Elements under Combined Normal Force and Bending, IABSE Reports of the Working Commissions*, Universita di Roma, Rome, Italy.

Ministry of Housing and Urbanism of Chile (MINVU), 2011. *Reinforced Concrete Design Code, Replacing D.S N 118, 2010, DS 60*, Santiago, Chile (in Spanish).

Monti, G., and Nuti, C., 1992. Nonlinear cyclic behavior of reinforcing bars including buckling, *Journal of Structural Engineering* **118**, 3268–3284.

Motter, C. J., Abdullah, S. A., and Wallace, J. W., 2018. Reinforced concrete structural walls without special boundary elements, *ACI Structural Journal* **115**, 723–733.

Moyer, M. J., and Kowalsky, M. J., 2003. Influence of tension strain on buckling of reinforcement in concrete columns, *ACI Structural Journal* **100**, 75–85.

New Zealand Society for Earthquake Engineering (NZSEE), 2017. *The Seismic Assessment of Existing Buildings: Technical Guidelines for Engineering Assessment. Part C5 – Concrete Buildings*, NZSEE, SESOC, NZGS, MBIE, and EQC, Wellington, New Zealand.

Oh, Y. -H., Han, S. W., and Lee, L. -H., 2002. Effect of boundary element details on the seismic deformation capacity of structural walls, *Earthquake Engineering & Structural Dynamics* **31**, 1583–1602.

Paulay, T., and Priestley, M. J. N., 1993. Stability of ductile structural walls, *ACI Structural Journal* **90**, 385–392.

Priestley, M. J. N., Calvi, G. M., and Kowalsky, M. J., 2007. *Displacement-Based Seismic Design of Structures*, IUSS Press, Pavia, Italy, 721 pp.

Priestley, M. J. N., and Kowalsky, J. M., 1998. Aspects of drift and ductility capacity of rectangular cantilever structural walls, *Bulletin of the New Zealand Society for Earthquake Engineering* **31**, 73–85.

Rodriguez, E. M., Ortiz, A., and Torres Matos, M. A., 2013. Diseño dísmico de muros de concreto to reforzado basado en desplazamiento, in *Congresso Nacional de Ingenieria Sismica*, 6–9 November, Boca del Rio, Mexico (in Spanish).

Rodriguez, M. E., Botero, J. C., and Villa, J., 1999. Cyclic stress-strain behavior of reinforcing steel including effect of buckling, *Journal of Structural Engineering* **125**, 605–612.

Segura, Jr., C. L., and Wallace, J. W., 2018. Impact of geometry and detailing on drift capacity of slender walls, *ACI Structural Journal* **115**, 885–895.

Shegay, A. V., Motter, C. J., Elwood, K. J., Henry, R. S., Lehman, D. E., and Lowes, L. N., 2018. Impact of axial load on the seismic response of rectangular walls, *Journal of Structural Engineering* **144**, 1–32.

Standards Australia/Standards New Zealand, 2001. *Steel Reinforcing Materials, AS/NZS 4671:2001*, Sydney, Australia/Wellington, New Zealand.

Standards New Zealand (NZS), 1999. *Concrete Structures Standard - The Design of Concrete Structures: Amendment 2*, *NZS 3101:1995 A2*, Wellington, New Zealand.

Standards New Zealand (NZS), 2006. *Concrete Strutures Standard Part 1 - The Design of Concrete Structures*, Wellington, New Zealand.

Standards New Zealand (NZS), 2008. *Concrete Structures Standard Part 1 - The Design of Concrete Structures: Amendment No. 2*, Wellington, New Zealand.

Standards New Zealand (NZS), 2017. *Concrete Structures Standard: Amendment 3*, *NZS 3101:2006*, Wellington, New Zealand.

Su, R. K. L., and Wong, S. M., 2007. Seismic behaviour of slender reinforced concrete shear walls under high axial load ratio, *Engineering Structures* **29**, 1957–1965.

Tran, T. A., and Wallace, J. W., 2015. Cyclic testing of moderate-aspect-ratio reinforced concrete structural walls, *ACI Structural Journal* **112**, 653–666.

Wallace, J. W., Massone, L. M., Bonelli, P., Dragovich, J., Lagos, R., Lüders, C., and Moehle, J., 2012. Damage and implications for seismic design of RC structural wall buildings, *Earthquake Spectra* **28**, S281–S299.

Wallace, J. W., and Orakcal, K., 2002. ACI 318-99 provisions for seismic design of structural walls, *ACI Structural Journal* **99**, 499–508.

Welt, T. S., 2015. Detailing for Compression in Reinforced Concrete Wall Boundary Elements: Experiments, Simulations, and Design Recommendations, Ph.D. Thesis, University of Illinois at Urbana-Champaign, Urbana, IL.

(Received 1 August 2018; Accepted 4 February 2019)